*Article*

# Mechanical and Microstructural Properties of Composite Mortars with Lime, Silica Fume and Rice Husk Ash

**Ramalingam Malathy** [1,†] [iD], **Ragav Shanmugam** [1], **Ill-Min Chung** [2,†], **Seung-Hyun Kim** [2] and **Mayakrishnan Prabakaran** [2,*] [iD]

1   Department of Civil Engineering, Sona College of Technology, Salem 636 005, Tamil Nadu, India; malathycivil@sonatech.ac.in (R.M.); s.ragav1995@gmail.com (R.S.)
2   Department of Crop Science, College of Sanghuh Life Science, Konkuk University, Seoul 05029, Korea; imcim@konkuk.ac.kr (I.-M.C.); kshkim@konkuk.ac.kr (S.-H.K.)
*   Correspondence: prabakarannitt@gmail.com or prabakaran@konkuk.ac.kr
†   These authors contributed equally to this work.

**Abstract:** A mixture of hydraulic lime and pozzolanic material can be used as a binder in making concrete and mortar for energy-efficient construction purposes. Generally, lime possesses lower strength and higher setting time. By introducing pozzolans in the lime mortar, their cementitious properties could be increased and could compete with the cement mortars. The use of pozzolan-lime binder in mortar reduces the utilisation of cement, and hence reduces the environmental problem originating from cement production. This study mainly deals with the mechanical and microstructural properties of lime and lime composite mortars made up of hydraulic lime, silica fume and rice husk ash. Three composite mortars were made with the following combination such as hydraulic lime-silica fume (LSF), hydraulic lime-rice husk ash (LRA) and hydraulic lime-silica fume-rice husk ash (LSR). Further, their properties were compared with the pure lime mortar. Preliminary investigations were made on the lime reactivity and pozzolanic reactivity tests. It was understood that silica fumes have a (15%) better reactivity than rice husk ash. The introduction of pozzolans in the lime mortar promotes fresh, hardened and microstructural properties. The 28 days' compressive strength of lime composite mortars achieved more than 16 Mpa, while the lime mortar attained 4 Mpa. The combined effect of pozzolanic reaction, hydration and carbonation in the lime composite mortars achieved four times the strength of lime mortar at 28 days. A high peak of calcium carbonate was detected in lime mortar as a result of carbonation. The well-developed microstructure of calcium silicate hydrate and calcium hydroxide exhibits the formation of hydration products in the lime composite mortars as observed from a scanning electron microscope (SEM), energy-dispersive X-ray (EDX) and X-ray diffraction (XRD). Similar graphs of Fourier transform infrared spectroscopy (FT-IR) showed the presence of equivalent functional elements in all lime composite mortars.

**Keywords:** hydraulic lime; silica fume; rice husk ash; reactivity; microstructure; SEM; EDX; XRD; FT-IR

## 1. Introduction

Lime mortar is a binder that was mainly used in olden days for stone and brick masonry. Lime was mixed with many natural organic materials such as Jaggery, Kadukkai, Egg white, curd, Bel pulp, lentils, etc., to form a strong and workable mortar [1–4]. However, the preparation procedures for many traditional binders were dismembered and unknown due to the major use of Portland cement in construction activities from the 19th century [5,6]. At present, lime mortar is used only for the purpose of conservation of old historic structures and temples. The current scope of lime mortar in addition to pozzolanic material could increase strength and decrease setting time due to the formation of calcium silicate hydrate (C-S-H) gel. Addition of pozzolan with lime in the presence of water would lead to the natural formation of C-S-H gel [7–9]. This is the main reaction product for strength

production in Portland cement. In cement manufacturing, carbon dioxide is emitted during the heating process and energy is utilised in the form of fuel. Hence, to reduce pollution and conserve the environment, cement usage can be reduced by the addition of low-carbon alternative material [10–12]. Lime is a naturally available material produced from limestone that can replace the role of cement mainly for mortar usage.

Lime exhibits slow setting time and strength gain compared with cement mortar. In pure lime, setting and strength gain is achieved by the carbonation process, i.e., conversion of calcium hydroxide ($Ca(OH)_2$) into calcium carbonate ($CaCO_3$) in the presence of carbon dioxide in air. However, in cement, setting and strength gain is achieved by the hydration process, i.e., reaction between bogue compounds present in the cement and water. The influence of hydraulic lime content on the properties of blended aerial lime-hydraulic lime mortars up to 75% was studied. A moderate increment of compressive strength and significant decrease in the pore structure at higher substitution of hydraulic lime was observed [5]. The effect of curing conditions on lime mortar was studied with the addition of two pozzolanic materials such as metakaolin and zeolite. Four types of curing conditions were used, such as saturated curing (RH 100%), air curing (RH 65%), carbonation chamber curing ($CO_2$) and combined humid and air curing (RH 100/65%). The compressive strength of lime-metakaolin mortar achieved 12 MPa at 365 days and saturated curing (RH 100%) showed the most suitable curing condition on the entire process [9]. The addition of rice husk ash (RHA) in the hydrated lime mortar increased the strength only at a low-level replacement of lime. RHA lowered the water demand of hydrated lime mortar but increased the water demand of cement composites. The addition of RHA densified the microstructure of lime mortar with needle-like hydrates [13].

Masonry mortar with equal amounts of cement and lime exhibits a dense spherical microstructure without any acicular forms (needle-like hydrates). However, when 10% of silica fume was added in replacement with the cement in the mortar, acicular microstructure was formed at later ages due to the pozzolanic reaction between the silica fume and lime [14]. The use of lime kiln dust (LKD) as a cementitious material in mortar increases the water demand, reducing the strength and density of the mortar. Hence, it should be used at minor replacements [15]. The effects of mineral addition on binary and ternary combinations with hydraulic lime mortar were studied using silica fume, ground granulated blast furnace slag (GGBS), fly ash, English red brick dust (ERBD), Italian red brick dust (IRBD) and three forms of metakaolin. Saturated curing and air curing of 65% relative humidity at 20 °C were performed. In that, the ternary combination of hydraulic lime, silica fume and GGBS showed the highest strength in both curing conditions. Saturated curing is more suitable than air curing for the lime mortar with the usage of pozzolans [16].

Three types of lime–pozzolan–cement mixes after exposure to the high temperature of 8000 °C were investigated with fly ash and hydrated lime. The conventional mix (P-L) was made up of 80% fly ash and 20% hydrated lime; alkali-activated mix (P-A) was made up of 76.8% fly ash and 19.2% hydrated lime with 4% of sodium sulphate solution as an activator; hybrid alkali-activated mix (P-H) was made up of 30% cement, 53.76% fly ash and 13.44% hydrated lime with 2.8% of sodium sulphate solution. Higher strength development was observed in P-H pastes than others due to the early strength development of cement and pozzolanic effect with the fly ash and free $Ca(OH)_2$ from cement. SEM and XRD analysis at 7 and 28 days showed that no hydration products were observed in the conventional mix. The addition of activator solution and Portland cement in the other mixes increased the microstructure growth as well as the formation of new hydrates in it [17]. Microstructural properties of lime (L) and lime-pozzolan (LP) paste were studied with the addition of 1.5% of nanosilica (NS) in the pastes. An equal amount of natural pozzolan of volcanic origin was used in the LP paste. The addition of NS increased both the compressive and flexural strength of L paste and only the compressive strength in LP paste. SEM analysis showed that the L paste had porous, sphere and plate-like crystals due to the carbonation of lime. When addition of NS in L paste leads to the formation of new needlelike crystals due to pozzolanic reaction. LP paste exhibits the denser structure than L paste and the needle-like

hydration products were also formed due to the pozzolanic reaction between the lime and natural pozzolan. This was further increased with addition of NS in the LP paste [18].

When fly ash (FA) and rice husk ash (RHA) were added into the Portland cement mortar at different replacements, the optimal percentage of RHA-FA in cement mortar was identified as 15%, and at higher replacements mechanical properties were declined. SEM images of all mortars exhibit the similar microstructure of C-S-H, portlandite and ettringite [19]. The effect of different sizes of aggregates on the properties of natural hydraulic lime (NHL 5 and NHL 3.5) mortars were studied with three mixes of fine (M2), medium (M1) and coarse (M3) aggregates on NHL 5 mortar, and one mix was made with medium (M4) aggregate on NHL 3.5 mortar. The use of coarse aggregates decreases the open porosity and increases the strength of NHL mortars. SEM analysis of 270-day-old mortars showed a well-developed microstructure with uniform grain distribution of hydration products. M4 mortar exhibits a denser microstructure than others due to the fine grain size of NHL 3.5 [20]. Changes in the properties of cement-silica fume (30%) mix was observed with and without usage of limewater (LW) for mixing. Using LW as a mixing solution delayed both initial and final setting times and early strength. However, in later stages, the pozzolanic reaction between the silica fume and lime-mixed water results in more formation of hydration products and thus increases the strength of the pastes. The addition of silica fume decreases the level of portlandite in both limewater and normal water cement pastes [21].

By combining limestone and natural clay as a raw materials and heating up to 1450 °C in the kilns, cement is formed. This process liberates more carbon dioxide and needs more energy. Rather than going for natural clay materials, silica-rich industrial by-products such as silica fume, rice husk ash, fly ash, ground granulated blast furnace slag, etc., can be combined with naturally available lime to form a pozzo-lime binder used as an alternative to cement [1–21]. By using this, the utilisation of natural clay for cement and energy used for fuel can be conserved and the emission of carbon dioxide to the atmosphere is reduced. The results of such studies would directly benefit the construction industry and broader use of these types of low-carbon sustainable concrete/mortar.

Early-age strength and higher setting time were major impacts in lime-based mortar/concrete. Research should be carried out to reduce these issues, by adding mineral and chemical admixtures to make it an effective composite mortar/concrete. Hereby in this study, silica fume and rice husk ash were the two mineral admixtures used in the lime mortars. Further, their fresh, mechanical and microstructural properties were studied and compared with the pure lime mortar.

## 2. Materials and Methods

Hydraulic lime of high calcium content, according to the specification of IS 6932: 1973 [22] and IS 712: 1984 [23], was used throughout this work. Lime has a high initial and final setting time of 4.75 and 48 h. Silica fume and rice husk ash were the two pozzolans used in this study. Silica fume is the by-product from silicon alloy industries and it is a very reactive pozzolanic material due to its high silica content and fine particle size. It has particle size of average diameter 150 nm and Blaine fineness of 15,000 $m^2$/kg. Rice husk ash (RHA) is also an effective pozzolanic material obtained by burning rice husk in a controlled environment. To obtain RHA in the amorphous state, it should be burnt in a controlled environment rather than uncontrolled combustion, and optimum burning should be carried out between 500 °C and 700 °C for 12 h [24,25]. Countries where rice production is abundant can effectively use rice husk ash in mortar/concrete to reduce the cement content. Ordinary Portland cement of grade 53 with the specific gravity of 3.13 according to the specification of IS 269:2015 [26] and M-Sand passing through a 4.75 sieve with a specific gravity of 2.69 according to the specification of IS 383:1970 [27] were used. Physicochemical properties of materials used in the mortar are given in Table 1. The fineness modulus (FM) of the M sand used in our study is 3.39 and their gradation is given in Table 2.

**Table 1.** Physiochemical properties of materials.

| Property | Lime | Silica Fume | Rice Husk Ash |
|---|---|---|---|
| Colour | White | White | Off-white |
| Specific gravity | 2.74 | 2.63 | 2.25 |
| Bulk density | 687 kg/m$^3$ | 760 kg/m$^3$ | 480.2 kg/m$^3$ |
| SiO$_2$ | 1.00% | 99.88% | 88.90% |
| Al$_2$O$_3$ | - | 0.043% | 2.500% |
| Fe$_2$O$_3$ | - | 0.040% | 2.190% |
| CaO | 95% | 0.001% | 0.220% |
| MgO | - | 0.000% | - |
| K$_2$O/Na$_2$O | - | 0.001/0.003% | 0.69% |
| Cl | 0.01% | - | - |
| SO$_4$ | 0.20% | - | - |
| Pb | 0.001% | - | - |
| LOI | - | 0.015% | 4.01% |

**Table 2.** Gradation of M sand.

| IS Sieve | Weight Retained (gm) | Cumulative Weight Retained (gm) | % Cumulative Weight Retained | % Passing | Permissible Limit (IS 383-1970)% |
|---|---|---|---|---|---|
| 4.75 mm | 69 | 69 | 6.9 | 93.1 | 90–100 |
| 2.36 mm | 65 | 134 | 13.4 | 86.6 | 85–100 |
| 1.18 mm | 78 | 212 | 21.2 | 78.8 | 75–100 |
| 600 µm | 148 | 360 | 36 | 64.0 | 60–79 |
| 300 µm | 297 | 657 | 65.7 | 34.3 | 12–40 |
| 150 µm | 305 | 962 | 96.2 | 3.8 | 0–10 |
| Pan | 38 | 1000 | 100 | 0 | - |

Figure 1 shows that the XRD pattern of hydraulic lime exhibits the major mineral phase of calcium hydroxide and minor phase of calcium carbonate. Calcium carbonate was detected due to the presence of moisture in the surface of lime that reacts with the atmospheric air and is converted into thick granules. This can be removed by sieving, making it into fine powder and hydrating it to use for the mortar preparation. Figure 2 shows that the XRD pattern of silica fume exhibits the major mineral phase of quartz (SiO$_2$) and minor phase of cristobalite. The high peak between the 20° and 30° angle indicates the presence of amorphous silica in the material. Some amounts of crystalline silica (cristobalite) also detected may be due to the impurities present in the silica fume. Figure 3 shows that the XRD pattern of rice husk ash (RHA) exhibits a wide hump peak between the 20° and 30° angle, indicating the presence of amorphous silica [19,25]. Almost all the quartz present in the RHA is amorphous in nature.
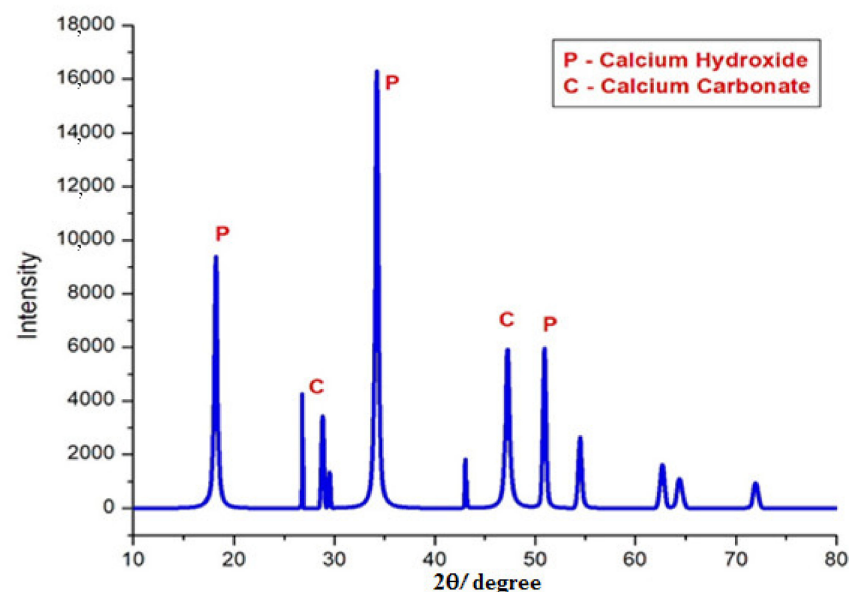


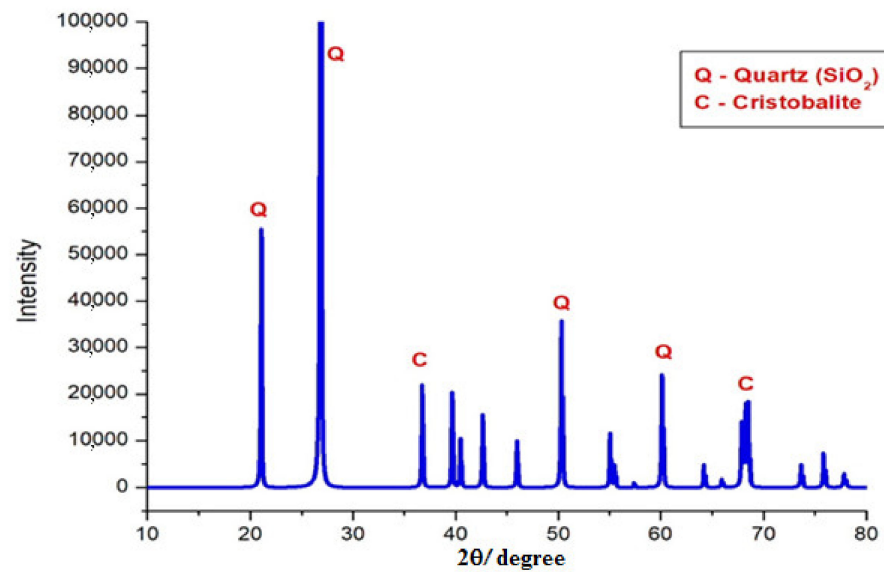**Figure 1.** XRD pattern of hydraulic lime.
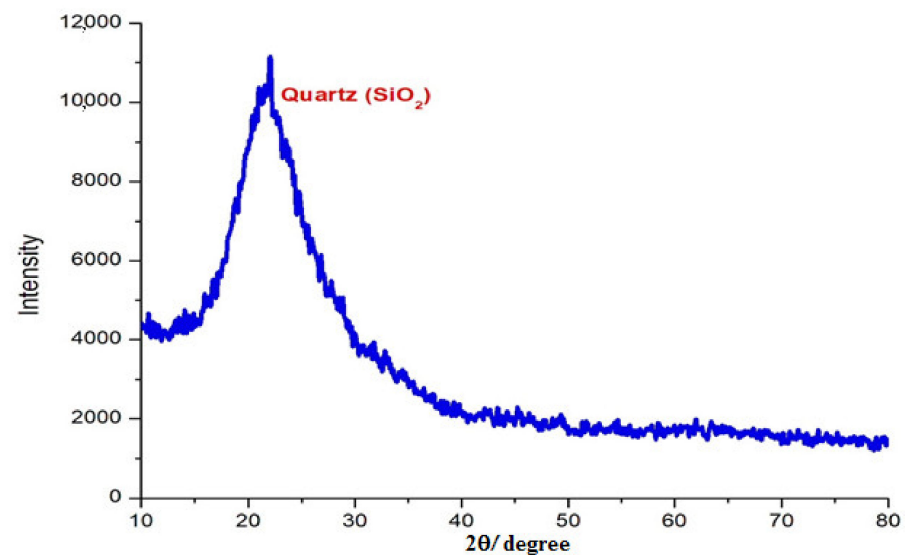
**Figure 2.** XRD pattern of silica fume.



**Figure 3.** XRD pattern of rice husk ash.

### 2.1. Methods

Mortars were prepared by hand mixing in the ratio of one part of binder with three parts of fine aggregate in accordance with IS 2250:1981 [28]. Equal amounts of lime and pozzolans were used in the mortar. Pure lime mortar was made for reference purposes. Around 20% of cement was added in the lime composite mortars. Addition of cement decreases both the initial and final setting time up to 50% and contributes in early strength development. Table 3 shows the mortar composition in parts by weight. The water-to-binder ratio was kept as 0.5.

**Table 3.** Ratio proportion of materials (percent).

| Mix ID | Cement | Lime | Silica Fume | Rice Husk Ash | M-Sand | Water |
|--------|--------|------|-------------|---------------|--------|-------|
| Li | - | 1 | - | - | 3 | 0.5 |
| LSF | 0.2 | 0.4 | 0.4 | - | 3 | 0.5 |
| LRA | 0.2 | 0.4 | - | 0.4 | 3 | 0.5 |
| LSR | 0.2 | 0.4 | 0.2 | 0.2 | 3 | 0.5 |

### 2.2. Lime Reactivity Index

The reactivity of the pozzolanic material with hydrated lime was determined by compressive strength of standard mortar cubes prepared and tested as per IS 1727:1967 [29]. The materials of the mortar were taken as lime: pozzolana: standard sand in proportion of 1:2M:9. 'M' represents the ratio of specific gravity of Pozzolana with the ratio of specific gravity of lime. Initially, lime and pozzolana were mixed thoroughly and sand was added with sufficient water. The water should be added to the mortar mixture until it reaches the flow of $70 \pm 5$ percent in the mortar flow table with 10 drops in 6 s. Then, the mortar cubes were casted and kept for 48 h. Gunny bag curing was provided for the mortar cubes and tested for 8 and 14 days.

### 2.3. Pozzolanic Strength Activity Index

As per ASTM C 311-05 [30] and ASTM C 1240-03a [31], mortar cubes were casted with the replacement of silica fume and rice husk ash with the cement. Their compressive strength was tested for 7 and 28 days. Binder-to-sand ratio should be taken as 2.75 and workability of test mortar should be ±5% of control mortar. Percentage increase in the strength of test mortar cubes containing pozzolans with the control mortar indicates the pozzolanic strength activity index of the pozzolans that we have used in our study.

$$\text{Strength activity index with Portland cement} = (A/B) \times 100$$

where A = average compressive strength of test mixture cubes (contains pozzolan), MPa and B = average compressive strength of control mix cubes, MPa.

### 2.4. Fresh Properties

Workability is one of the important properties of mortar. Mortar must be free enough to flow without any segregation of water or solid materials in the mix. However, addition of more water in mortar reduces its strength and bonding. Workability of mortar can be determined by mortar flow test. Mortar flow table had a diameter of 250 mm and a centre mould of base diameter 80 mm was placed. Well-mixed mortar was placed at the mould by two layers and damped 20 times. After two minutes, the mould was removed. Next, the table was dropped with the height of 12.5 mm for 25 times. Mortar flow diameter was measured at four directions and average is taken. The ratio between the flow diameter and base diameter gives the workability of the mortar in percentage. Density was determined by the ratio of weight of the mortar to the volume of the mortar cube. Density expresses the dead load of the structure. Fresh density and hardened density at 28 days curing of mortars were observed to understand the weight variations.

### 2.5. Compressive Strength

Mortar cube moulds of dimensions 70.5 mm × 70.5 mm × 70.5 mm were well-greased, and then mortar was placed as two layers; with each layer, damping was carried out 20 times with steel rod. After 48 h, samples were demoulded and taken for curing. Air curing was provided for lime mortar cubes and gunny bag curing was provided for lime composite mortar cubes to cure under by pozzolanic reaction as well as carbonation. Compressive strength test was performed for the mortar cubes on 7, 14 and 28 days of curing.

### 2.6. Drying Shrinkage

Drying shrinkage is the volumetric change in the concrete/mortar due to the capillary loss of the water in the pores of the concrete/mortar over the ages. This phenomenon leads to the internal warping and cracking on the surfaces of the concrete/mortar. Drying shrinkage depends on several factors such as material properties, proportions of the materials, type of mixing, water content, curing conditions, surrounding environment, etc. The drying shrinkage of mortar is determined by length comparator apparatus based

on IS: 4031-1988 (part 10) [32]. To measure the drying shrinkage, the mortar bars of size 25 mm × 25 mm × 250 mm were used. The mortar was made up of binder-to-sand ratio of 1:3 with the water content of 0.5 and compacted by hand compaction. Before pouring the mortar, gauge studs were inserted in the bar moulds coaxial with the bar, and they was greased well with oil. After 48 h, the mortar bar specimens were demoulded and their initial length was measured in the length comparator, as shown in Figure 4. Then, the specimen was taken for curing. Length of each specimen was measured using a length comparator immediately after taking it from curing. The length of the specimen was measured at different periods of 30, 60 and 90 days to calculate the drying shrinkage.
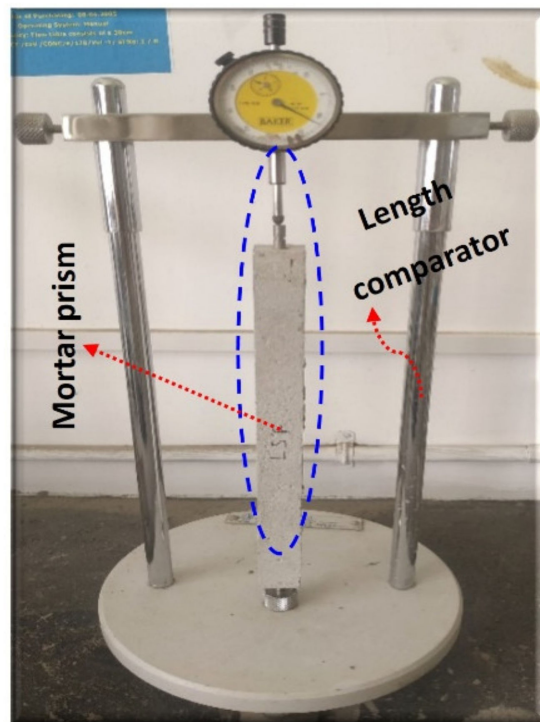


**Figure 4.** Length comparator test setup.

*2.7. Water Absorption*

The water-absorption test was carried out for the mortar cube specimens at 28 days of curing as per ASTM C 642-06 [33]. At the end of 28 days, mortar cubes were taken from gunny bags and placed in an oven for 48 h at a temperature of 105 ± 5 °C. Then, oven-dried specimens were cooled in atmospheric conditions and specimens were weighed (Wd). Cooled specimens were immersed in a tank containing potable water for another 48 h. Each specimen was removed from the water tank and wiped with a cloth to remove the surface water and weighed again (WS). The change in weight with the original weight expresses the water absorption of the concrete/mortar in percentage.

*2.8. Microstructural Properties*

The mortar samples of 7 and 28 days of curing ages were taken. Then, they were powdered and sieved through 75 µm and were taken for microstructural analysis. Scanning electron microscope (SEM) analysis was carried out with the ZEISS microscope with the VPSE G3 signal detector at various magnifications to determine the internal structure. Energy-dispersive X-ray (EDX) analysis was performed for the samples after examining SEM to analyse their chemical compositions, at an acceleration voltage of 10 keV [34–38]. To study the hydrated products and mineral phase in the mortar, X-ray diffraction was performed. The XRD pattern was observed by scanning the samples between 10 and 80 2θ range with an increment of 0.01 count and with a voltage of 40 MV by using a vertical X-ray diffraction meter [39–41]. FTIR spectroscopy was performed for the mortar samples to

observe the similarities in the functional group of the elements present in it. Samples were examined under attenuated total reflection (ATR) mode between the range 4000–400 cm$^{-1}$ with a spectral resolution of 4 cm$^{-1}$ [42,43].

## 3. Results and Discussions

### 3.1. Lime Reactivity Index

The reactivity of lime with silica fume (Li-SF) and rice husk ash (Li-RHA) were observed by testing their mortar cubes at 8 and 14 days. At both curing ages, lime with silica fume mortar exhibits a higher strength than RHA, as shown in Figure 5. This is due to the fine particles of the silica fume reacting well with lime under a short period. Moreover, the water requirement of Li-RHA mortar to reach the specified flow is much higher than the Li-SF mortar [13]. Due to the addition of more water, the Li-RHA mix setting time increased and the pozzolanic activity of the materials began late. More voids were observed in the Li-RHA mortar, which led to a reduced strength than Li-SF mortar. A continuous increase in strength of both Li-SF and Li-RHA mortar were observed as a result of pozzolanic reaction.
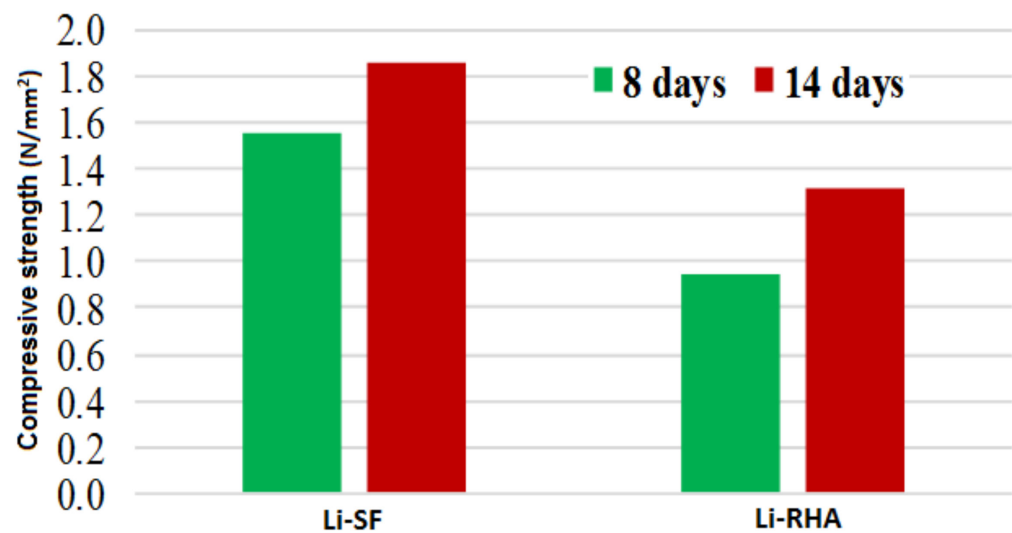


**Figure 5.** Lime reactivity test.

### 3.2. Pozzolanic Strength Activity Index

The ability of the pozzolanic materials such as silica fume and rice husk ash in contributing increase in strength of the cement mortar can be determined by the pozzolanic strength activity index. As per ASTM C 311-05 [29] and C 1240-03a [30], mortars were made with silica fume (SF) and rice husk ash (RHA). Due to the minor replacement, the water requirement of the SF mortar was similar with the control one but RHA mortar absorbed more water. At 7 and 28 days of curing, SF and RHA mortars exhibit more strength than control mortar as shown in Figure 6. This is due to the combined pozzolanic reaction and hydration of cement results in an increment of strength. At earlier stages of the pozzolanic reaction, the specific surface area of the pozzolans plays a main role in strength increase, while at later stages amorphous silica dominates the activation [44,45]. The pozzolanic strength activity index of SF mortar was 12% and RHA mortar was 11% higher than the control cement mortar. From this, SF mortar contributes to a higher strength than RHA mortar due to the high silica content, ease in mixing and finer size.
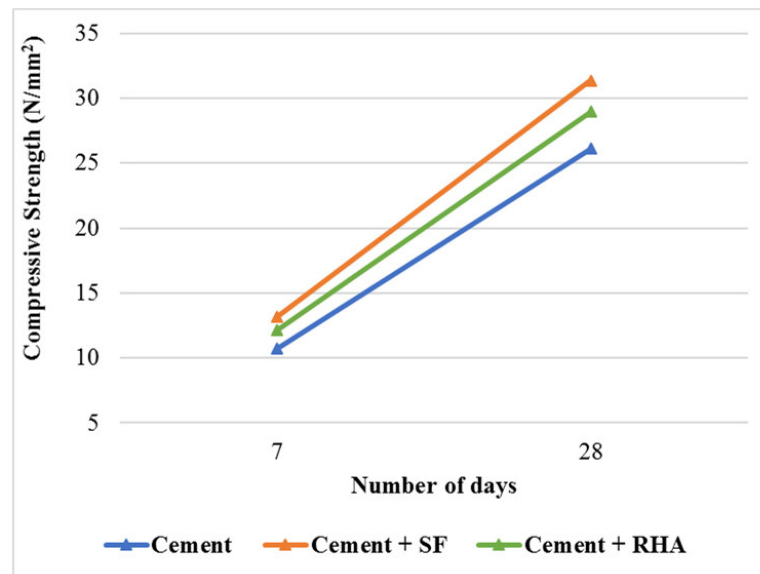
**Figure 6.** Pozzolanic strength activity test.

### 3.3. Fresh Properties

All mortar mixes have a common water-to-binder ratio of 0.5. Figure 7 shows the workability of mortars. The pure lime mortar gave the minimum flow of 52%, while the lime composite mortars were more workable than pure lime mortar. LSF mortar was more workable than others due to the fine spherical particles of silica fume being rolled in the water easily. RHA is fibrous in nature and it does not have the capacity to roll on. Generally, RHA has more water demand than cement and lower water demand than hydrated lime [45]. Hence, the combination of lime with pozzolans increases the workability of lime mortars. From Figure 8, both the fresh and hardened density of lime mortar was less than the lime composite mortars due to the low specific gravity. Although the specific gravities of silica fume and rice husk ash are less than the lime, they are finer and easily dispersible. The minor addition of cement fills the micropores of the mortar and increases the density. Finer pozzolans not only induce the pozzolanic activity, but also the particle-packing effect of the mixture [44].
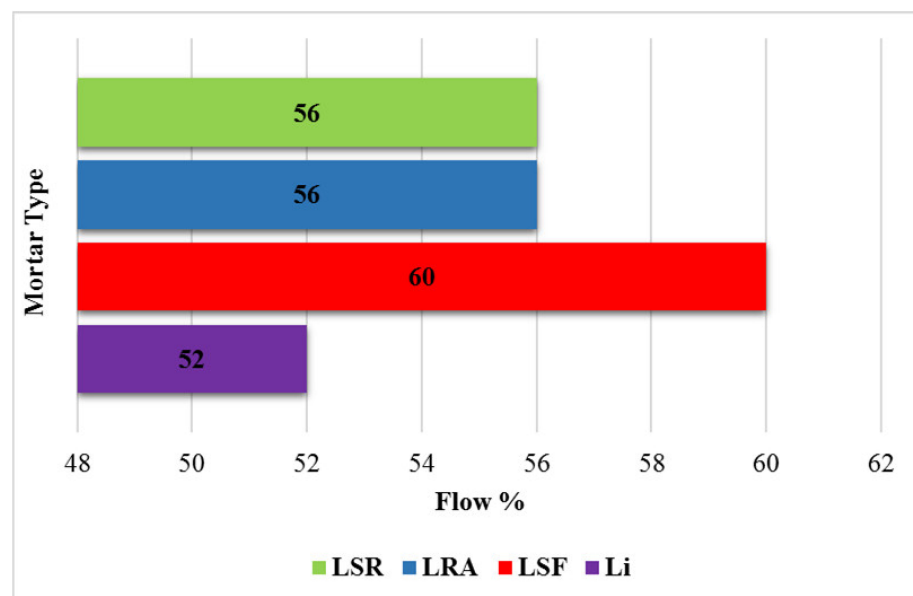


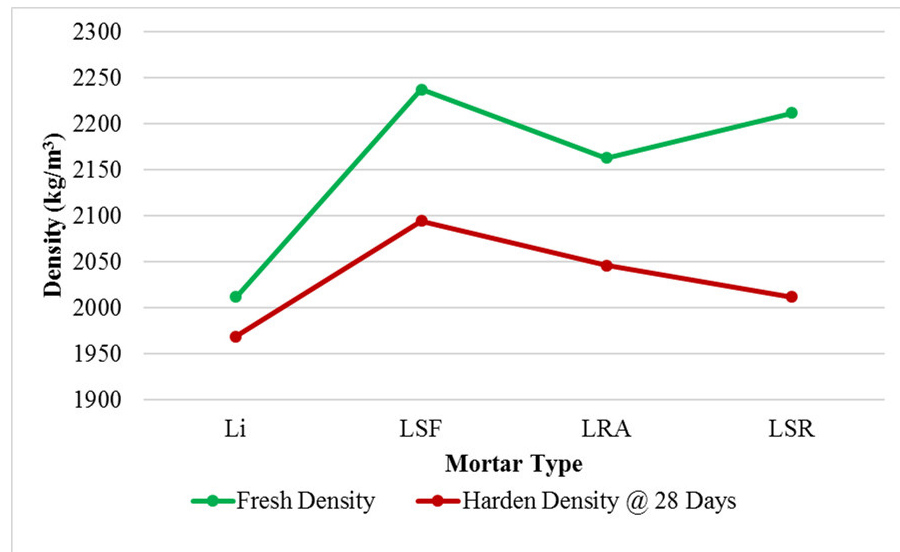**Figure 7.** Workability of lime and lime composite mortars.

**Figure 8.** Density of lime and lime composite mortars.

*3.4. Compressive Strength*

The compressive-strength test result showed that all lime composite mortars achieve nearly four times the strength of pure lime mortar at 28 days of curing. As per Figure 9, lime mortar exhibits a slow strength increase compared with the lime composite mortar. At 28 days, lime mortar has the strength of around 4 Mpa, while lime composite mortar achieves that strength within 7 days. Between 14 and 28 days of curing, all mortar attains twice their strength. Hence, for lime-related mortars, a major strength increase can be observed only after 14 days. However, for cement mortar, a major strength increment was observed at early stages due to the presence of tricalcium silicate (C3S). The increase in the strength of lime composite mortar is due to the pozzolanic reaction between the calcium in lime and active silica in pozzolans. The addition of cement increases the early strength attainment and provokes pozzolanic activity. Lime mortar achieves strength only by the carbonation process, which is slow in nature, and lime composite mortar achieves strength by pozzolanic reaction, hydration and carbonation. Based on ASTM C270 [46], lime composite mortars (LSF, LRA, LSR) can be used in structural works such as retaining walls, masonry foundations, manholes, etc.
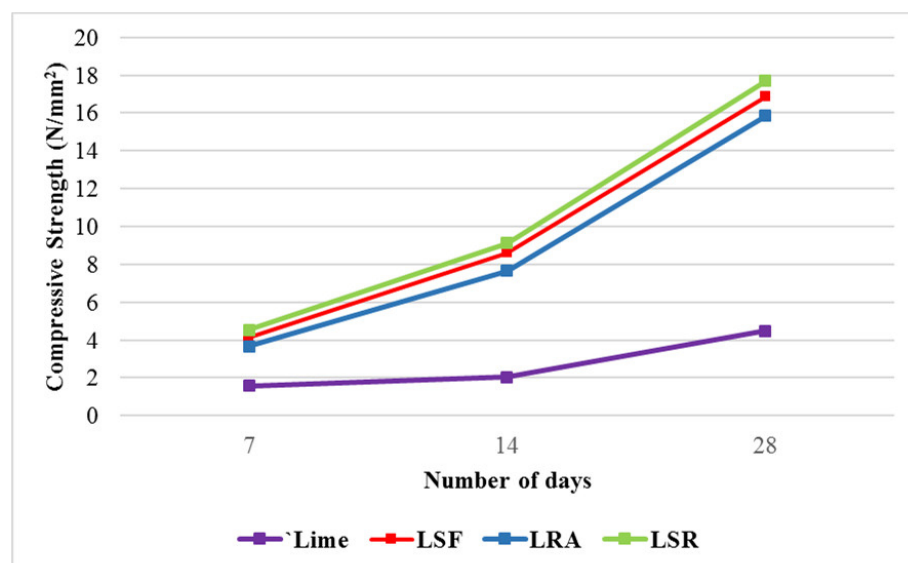


**Figure 9.** Compressive strength of lime and lime composite mortars.

### 3.5. Drying Shrinkage

Figure 10 shows the result of drying shrinkage of lime and lime composite mortar bars. It was observed that the lime mortar bar exhibits higher shrinkage than others. Carbonation of lime is initiated after the hardening of lime mortar leads to surface voids [44–54]. Lime composite mortar undergoes less shrinkage due to the formation of hydration products as a result of pozzolanic activity and hydration. Due to the higher water-to-binder ratio, the mortar undergoes shrinkage on their surface, leading to the formation of voids after drying [11]. Rice husk ash released excess water on the surface after compacting due to its hygroscopic nature, and when the water dried, micro surface voids were formed. In silica fume mortars (LSF and LSR), the surface voids were not much observed due to the lower water absorption than RHA. The fine particle size of the silica fume mixes well with the other materials and reduces the pores.
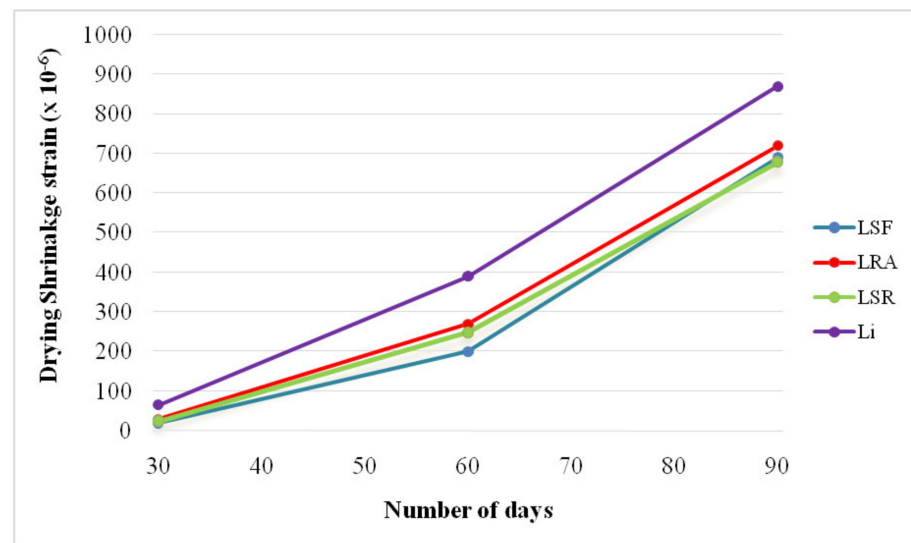


**Figure 10.** Drying shrinkage of lime and lime composite mortars.

### 3.6. Water Absorption

Figure 11 shows the saturated water-absorption percentage of the lime and lime composite mortars at 28 days. Lime mortar exhibits more water absorption than lime composite mortars. This was because lime mortar kept under air curing for carbonation with the atmospheric air, leading to the small pores in the surface and when immersed, the water was percolated into the pores. In lime composite mortars, the mix that contained maximum RHA content (LRA) absorbed more water than the silica fume. This is due to the fact that the rice husk ash absorbs more water while mixing for flowability and releases the excess water during the pozzolanic reaction [45–48]. Hence, small pores are created in the surface of mortar after the evaporation of released water. At higher curing ages, RHA absorbs less water because of the complete utilisation of active silica and therefore the reduction of permeable voids in it [47–54]. At a saturated condition, water penetrated through these pores and filled up the voids. Thus, water absorption was higher in the LRA and LSR mortars than LSF mortar.
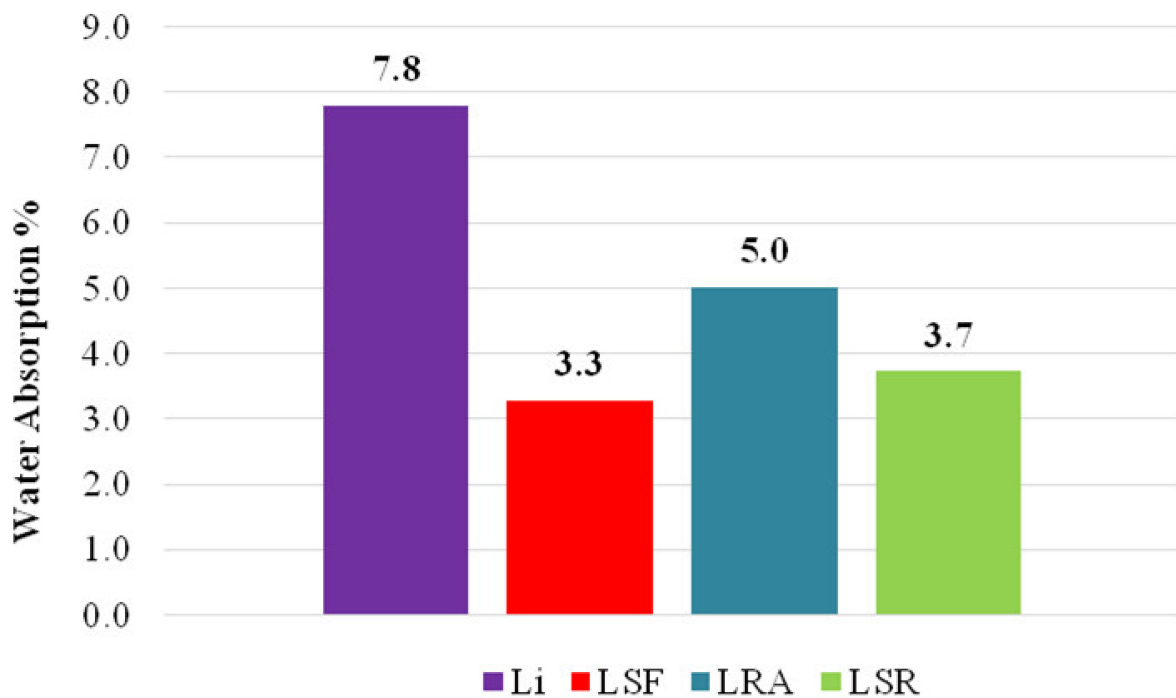
**Figure 11.** Water absorption of lime and lime composite mortars.

*3.7. Microstructural Properties*

3.7.1. SEM/EDX

Figures 12–15 show the SEM and EDX of lime and lime composite mortars. The SEM images of all lime composite mortars exhibits a maximum density of the spherical microstructure at both 7 and 28 curing days, while the SEM images of lime mortar do not have any hydrate growth and only the thick white calcium carbonate granules were viewed [47–54]. As per EDX, lime has an increasing content of calcium from 7 to 28 days as a result of carbonation. As per Table 4, EDX data of lime composite mortar showed an increase in silica content, and decrease in calcium content from 7 days to 28 days relates to the formation of hydration products in the mortar as a result of pozzolanic reaction. Due to the higher magnification, small fibrous rice husk ash particles were viewed in LRA and LSR mortar. However, in LSF mortar, silica fumes could not be differentiated due to their fine particle size. The wide spread of hydrates and compact microstructure without any voids were observed in the LSR mortar than other lime composite mortars. In pure lime mortar, an irregular microstructure and a large number of voids were observed. This was responsible for the low strength developed than other composite mortars. Since carbonation is a slow process, the microstructure growth goes on developing at latter stages. Overall, the lime composite mortar exhibits the dense spherical hydrates (Type III -CSH) [14,18,47–54]. There was no formation of acicular and hexagonal CSH morphologies found in the samples.
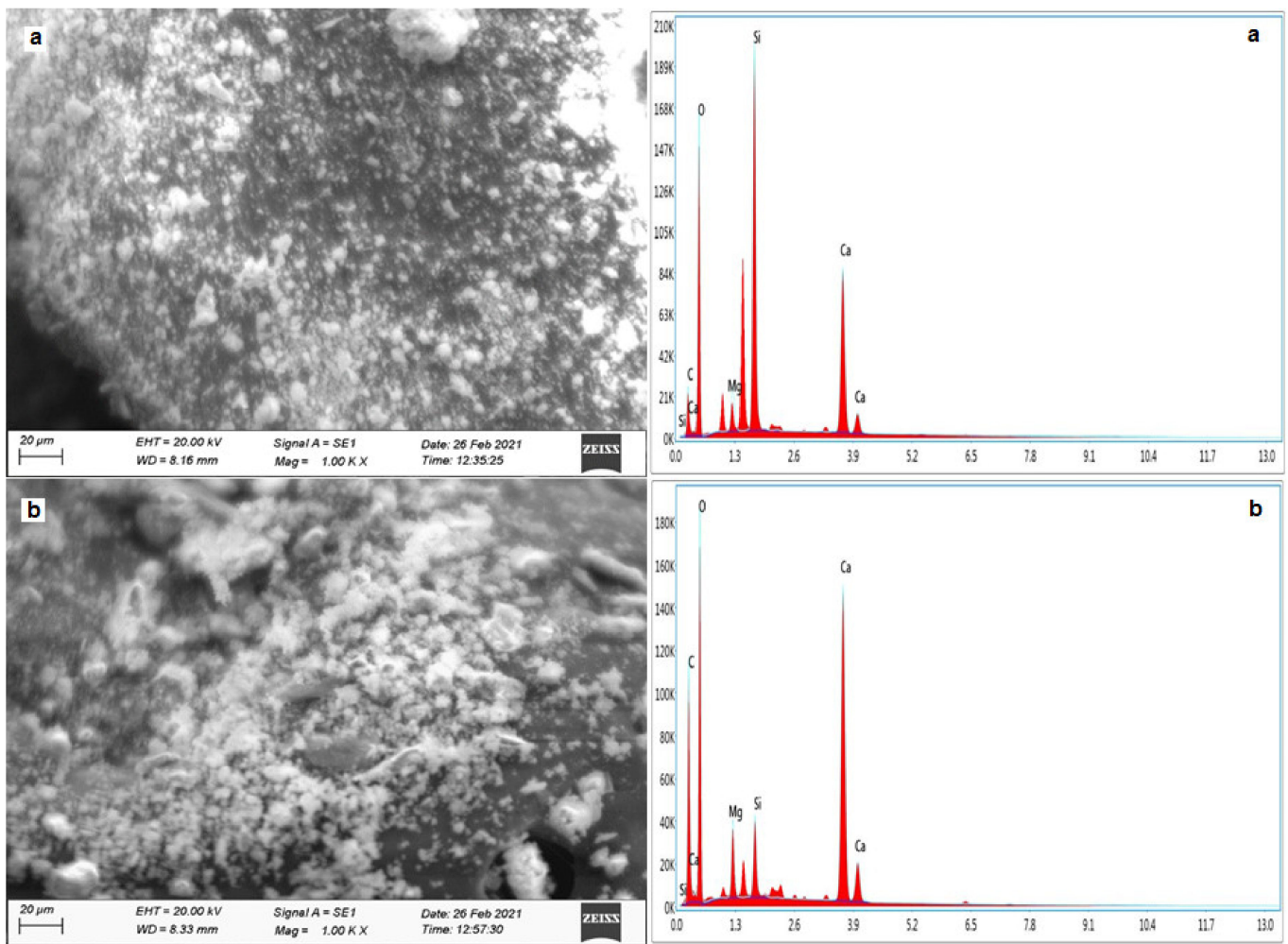
**Figure 12.** SEM and EDX result of lime mortar. (**a**) 7 days and (**b**) 28 days.

**Table 4.** EDX data of lime and lime composite mortars.

| Elements | Weight (%) | | | | | | | |
|---|---|---|---|---|---|---|---|---|
| | Lime | | LSF | | LRA | | LSR | |
| | 7 Days | 28 Days | 7 Days | 28 Days | 7 Days | 28 Days | 7 Days | 28 Days |
| Calcium | 23.07 | 29.89 | 15.41 | 14.29 | 23.36 | 11.32 | 30.26 | 18.06 |
| Silica | 20.7 | 3.11 | 14.53 | 17.57 | 10.72 | 11.55 | 24.27 | 11.80 |
| Carbon | 7.48 | 16.39 | 9.14 | 7.05 | 8.41 | 24.23 | 36.69 | 7.80 |
| Oxygen | 46.54 | 47.07 | 55.58 | 55.13 | 52.85 | 49.61 | 1.15 | 57.46 |
| Magnesium | 2.22 | 3.54 | 1.78 | 1.24 | 1.32 | 1.98 | 1.75 | 2.81 |
| Aluminium | - | - | 1.94 | 2.19 | 1.03 | 0.68 | - | 0.89 |
| Sulphur | - | - | 0.42 | 0.62 | 0.61 | 0.42 | 2.58 | 0.48 |
| Ferrous | - | - | 1.19 | 0.70 | 1.70 | 0.22 | 1.59 | 0.70 |
| Sodium | - | - | - | 1.22 | - | - | - | - |
| Titanium | - | - | - | - | - | - | 1.72 | - |
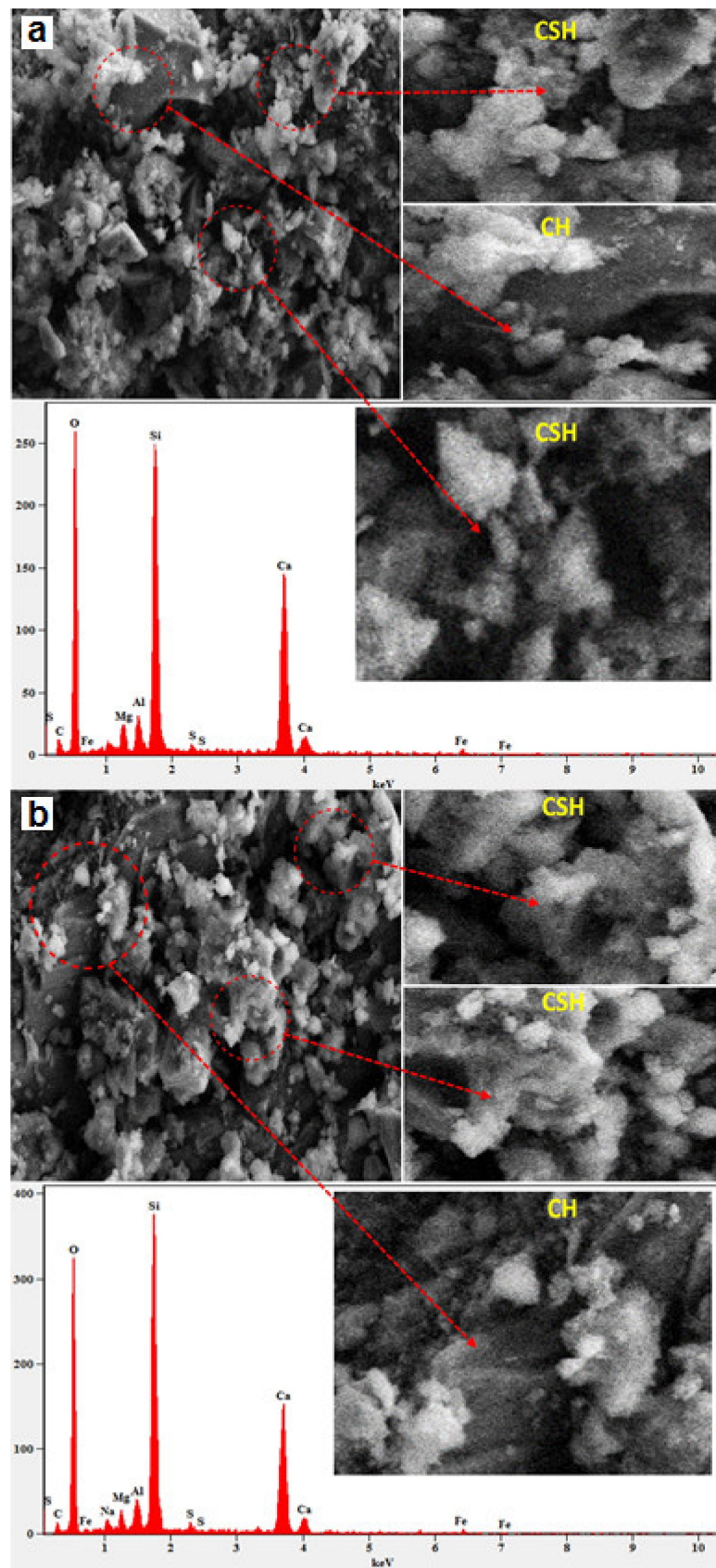
**Figure 13.** SEM and EDX result of LSF mortar. (**a**) 7 days and (**b**) 28 days.
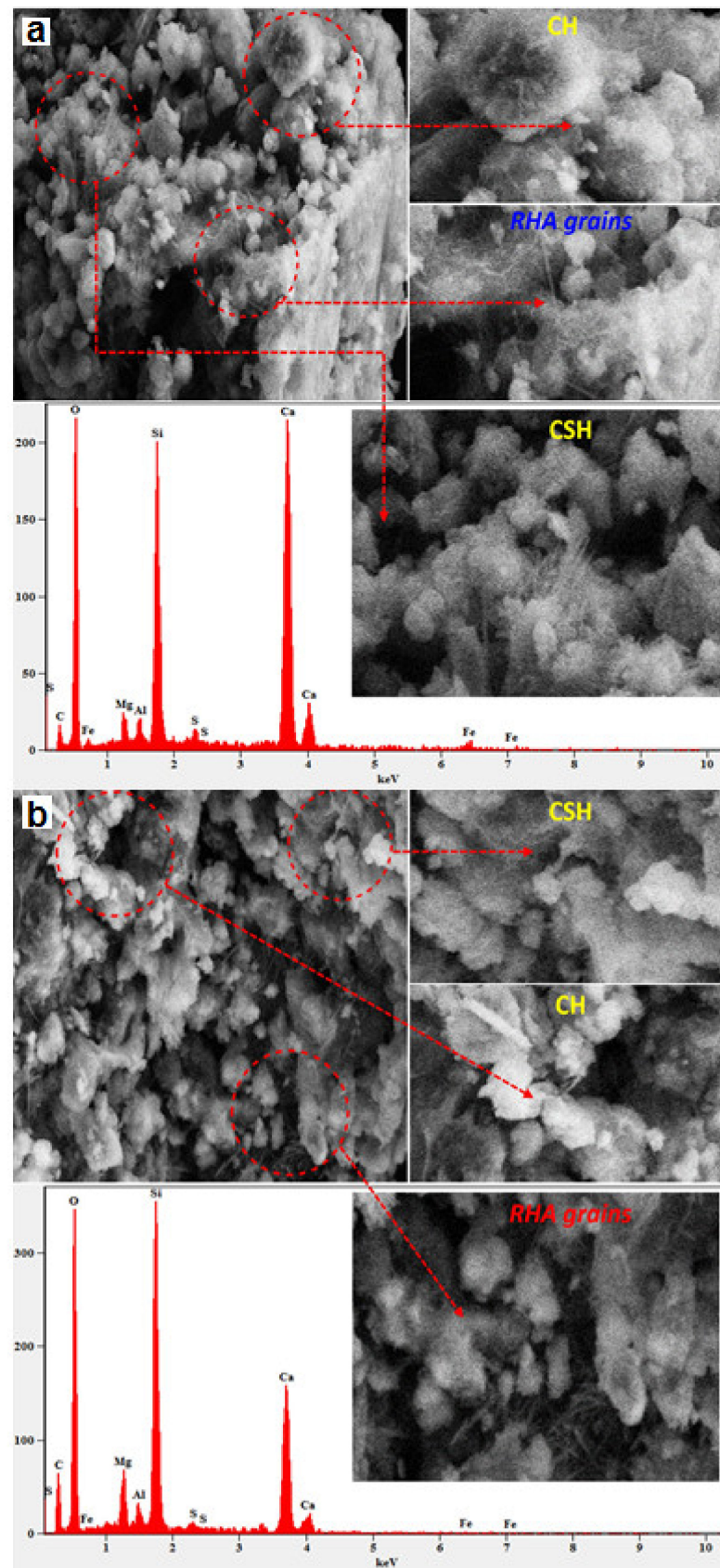
**Figure 14.** SEM and EDX result of LRA mortar. (**a**) 7 days and (**b**) 28 days.
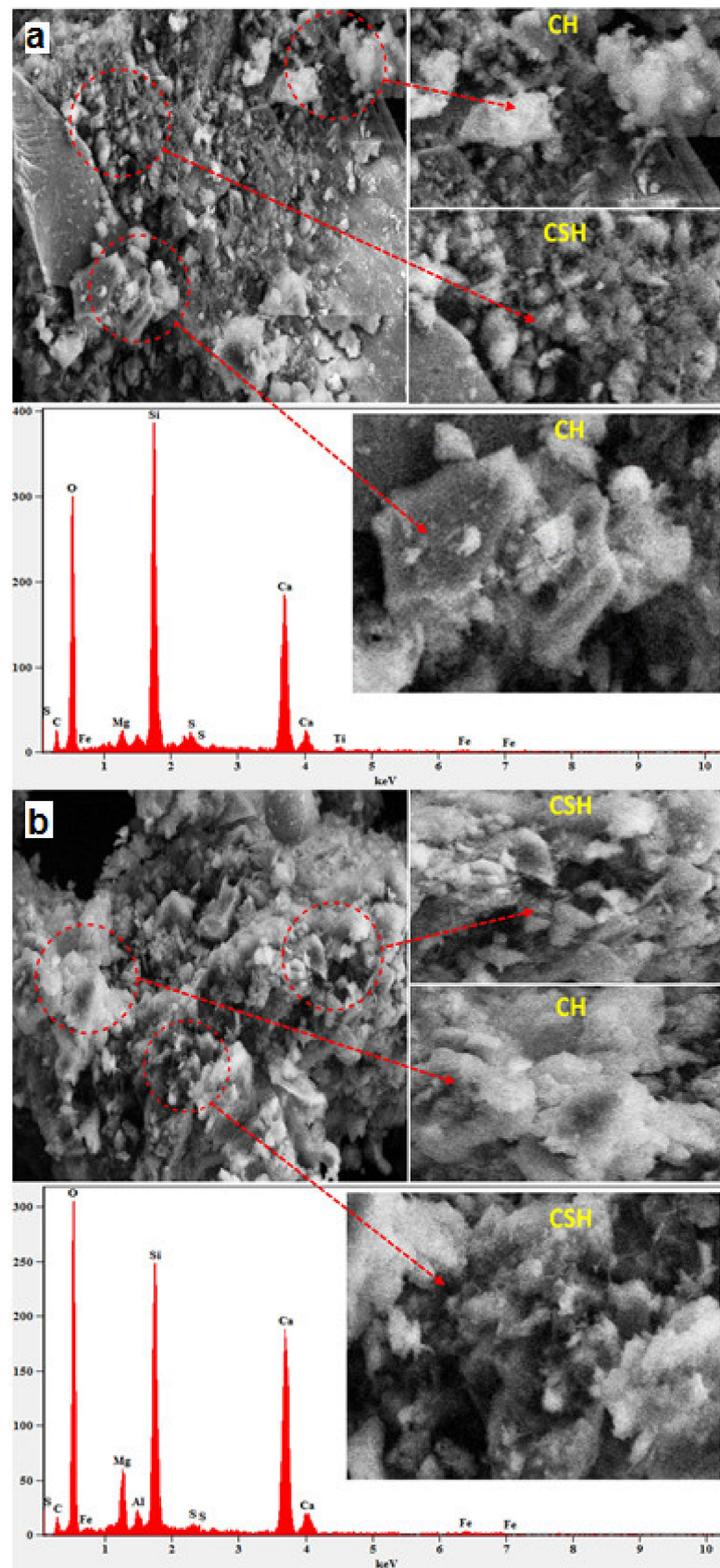
**Figure 15.** SEM and EDX result of LSR mortar. (**a**) 7 days and (**b**) 28 days.

### 3.7.2. XRD

XRD patterns of lime and lime composite mortars are shown in Figures 16–19. As a result of carbonation, calcium carbonate was the main product observed in the lime mortar [6]. Since carbonation is a long process, not all of the calcium hydroxide was converted into carbonate. Hence, calcium hydroxide was also observed in the sample. Quartz represents the inert silica present in the fine aggregate of the lime mortar. In all lime composite mortars, quartz ($SiO_2$) shows the maximum peak, indicating the use of effective pozzolanic materials and the use of siliceous fine aggregates in the mortar [7]. Hydrated products such as calcium silicate hydrate, calcium hydroxide and carbonated products such as calcium carbonate were identified in the samples. These related chemical reactions such as pozzolanic reaction, hydration and carbonation [6,9,10] took place in the lime composite mortars. Traces of dicalcium silicate (C2S) and tricalcium silicate (C3S) were found due to the addition of 20% cement in the mortar. High calcite peaks observed in the LRA mortar show higher carbonation than the other composite mortars. Well-distributed peaks of calcium silicate hydrate and small peaks of calcium hydroxide were identified in the LSR mortar representing the formation of more CSH and less CH as a result of pozzolanic reaction. Overall, the three lime composite mortars exhibit the similar mineral phases and no new mineral phase was identified. Minerals are formed as a result of pozzolanic reaction, hydration and carbonation favours strength increase in the mortars.
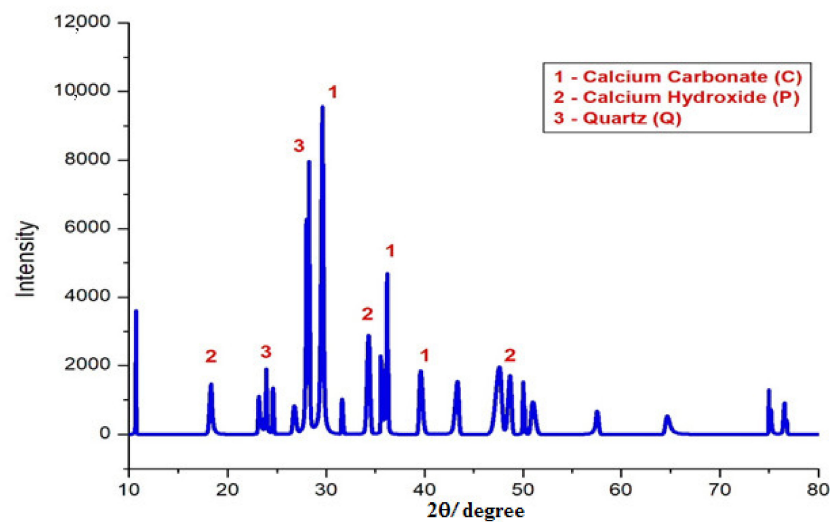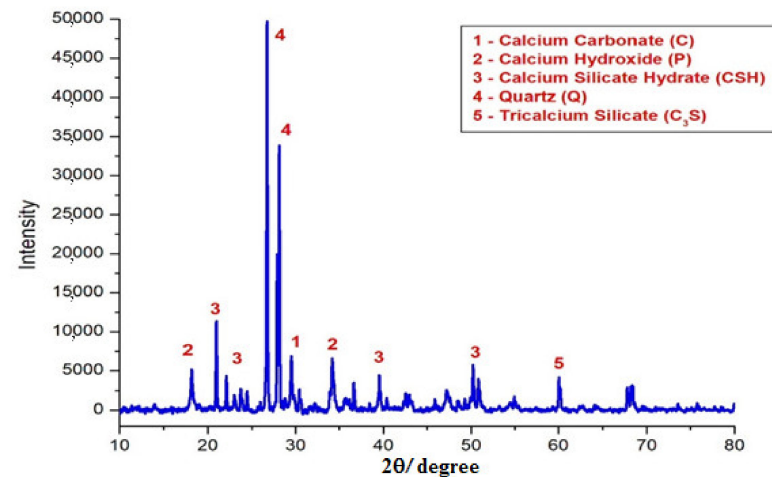


**Figure 16.** XRD pattern of lime mortar.



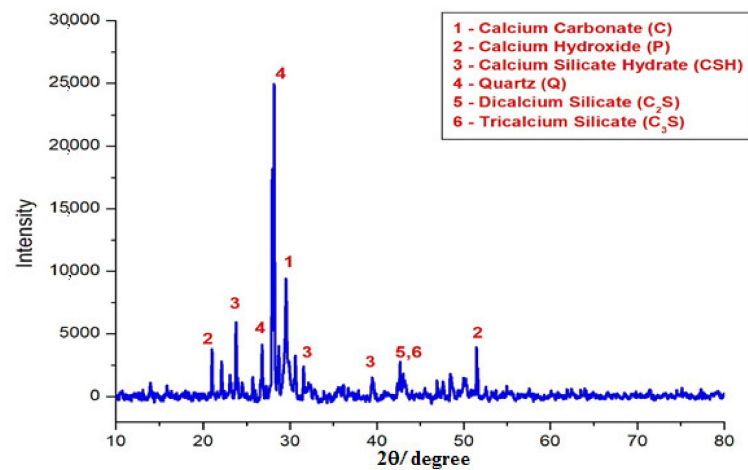**Figure 17.** XRD pattern of LSF mortar.

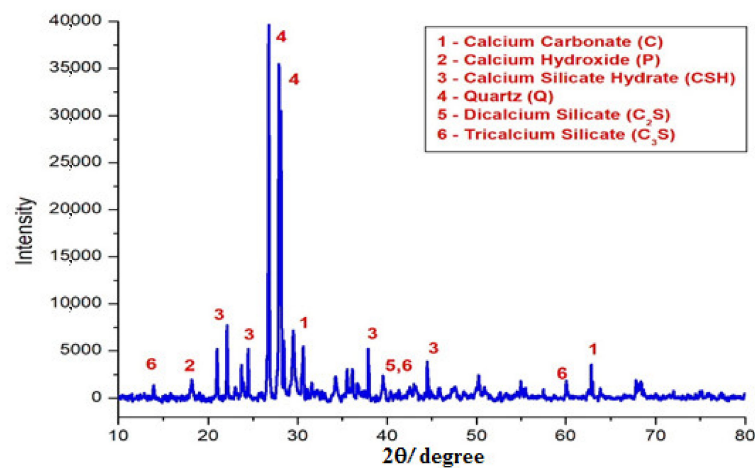**Figure 18.** XRD pattern of LRA mortar.



**Figure 19.** XRD pattern of LSR mortar.

### 3.7.3. FT-IR

Figures 20–23 show the FT-IR on the attenuated total reflection mode (ATR) pattern of samples Li, LSF, LRA and LSR, respectively. Figure 24 compares the FT-IR graph of all mortars. The strong asymmetric stretching in the range between 400 and 600 cm$^{-1}$ represents the Si-O bonds [19,55,56]. This indicates the presence of silica-oxygen bonding in the mortar. The strong asymmetric bending at 900–1100 cm$^{-1}$ represents the formation of hydration products such as calcium silicate hydrate (C-S-H) in the lime composite mortars [55]. However, in pure lime mortar, there was no strong bending observed. This indicates that there were no hydration products formed as a result of the pozzolanic reaction and hydration. Bending at 1400 cm$^{-1}$ represents the C-O phase and bending at 3300 cm$^{-1}$ represents the -OH phase due to the adsorbed water molecules in the mortar. Lime mortar was kept in atmospheric air curing for carbonation, and hence it does not have any adsorbed water. Strong bending at 3600 cm$^{-1}$ in lime mortar exhibits the presence of calcium phase (calcium carbonate) in the mortar. This bending was not observed in lime composite mortars because the calcium reacted with the silica to form hydrates. From Figure 23, it was observed that the FTIR pattern of lime composite mortars has similarities in stretching and bending to lime mortar.
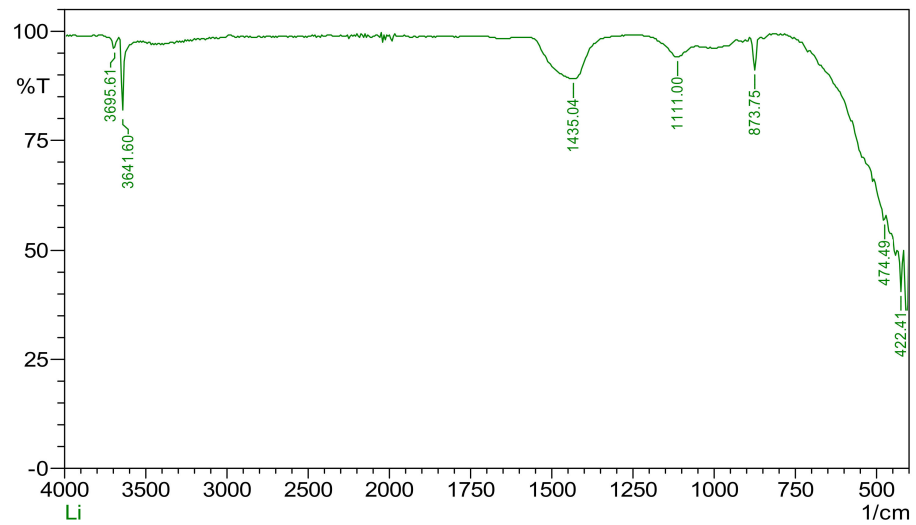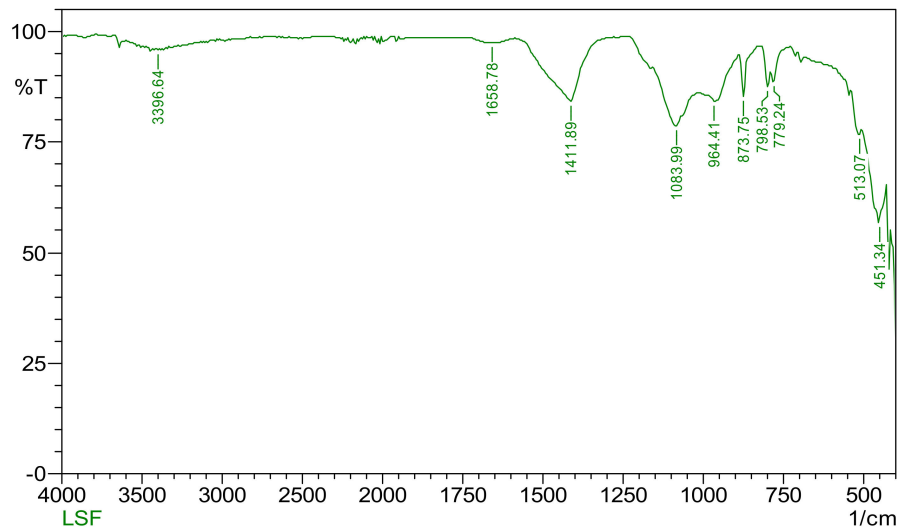
**Figure 20.** FTIR graph of lime mortar.



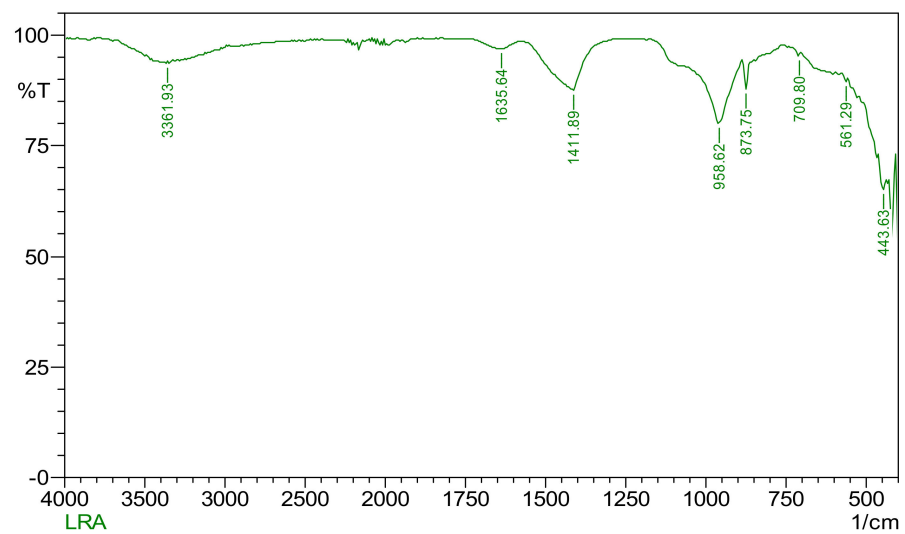**Figure 21.** FTIR graph of LSF mortar.


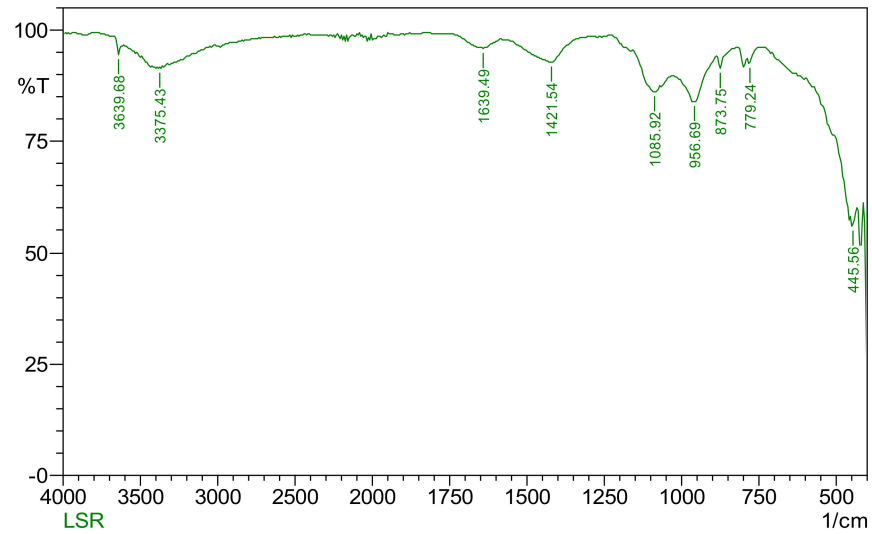
**Figure 22.** FTIR graph of LRA mortar.
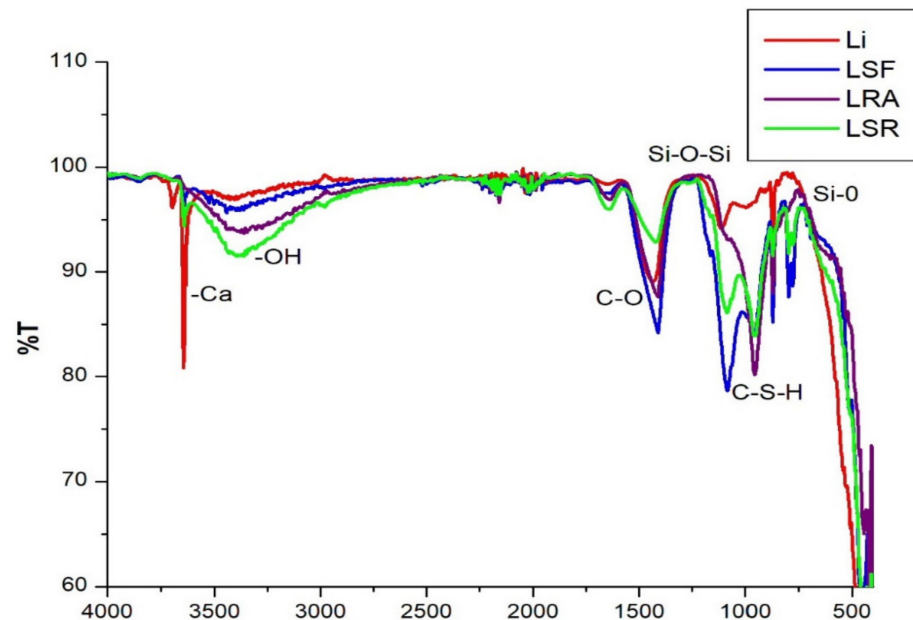
**Figure 23.** FTIR graph of LSR mortar.



**Figure 24.** Comparison of all FTIR graphs.
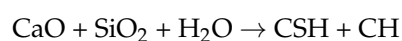
### 3.8. Mechanism

Cement possesses more than 60% CaO and about 30% $SiO_2$, which produces CH and CSH during hydration. Lime consists of more than 90% CaO, which can produce more CH. Pozzolans such as silica fume and rice husk ash contain more than 90% active $SiO_2$. When both lime and pozzolans are combined and in the presence of water ($H_2O$), they react to produce CSH and CH. This process is called a pozzolanic reaction.

Cement hydration:

Di/Tricalcium silicate + water calcium silicate hydrate + calcium hydroxide + heat

$$Ca_2SiO_4/Ca_3SiO_5 + H_2O \rightarrow CSH + CH + 173.6 \text{ kJ}$$
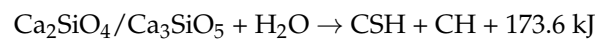
Lime-pozzolan hydration:

$$CaO + SiO_2 + H_2O \rightarrow CSH + CH$$

The mix should be designed suitably to produce more CSH and less CH based on different trials, as CSH is responsible for strength development in mortar/concrete. Figure 25 explains the complete diagrammatic reaction mechanism of lime composite mortar.
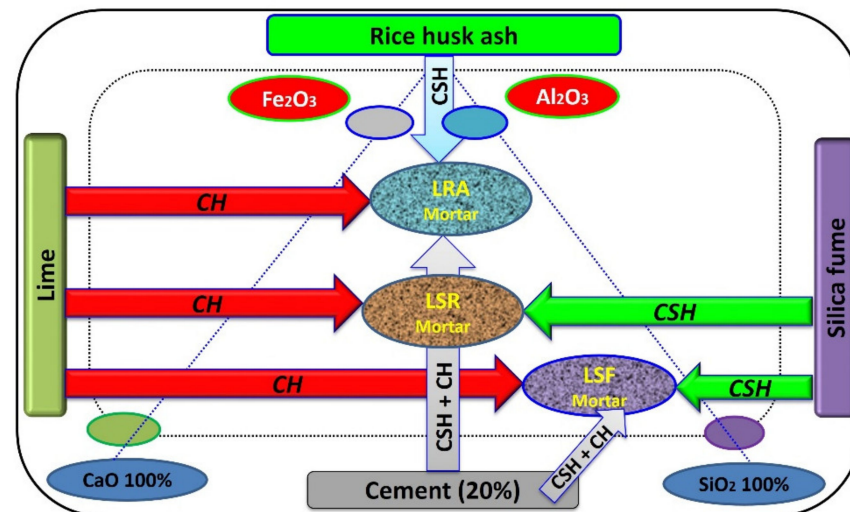


**Figure 25.** Mechanism of lime composite mortars.

## 4. Conclusions

Based on the results and discussions of this study, the conclusion is as follows:

➢ The addition of pozzolans as a replacement of lime in lime composite mortar has a positive effect on all mechanical and microstructural properties of mortar. From the lime reactivity test, it is understood that lime attains a cementitious property when it is added with pozzolans. The reactivity of silica fume and rice husk ash as determined from the pozzolanic strength activity index showed that silica fume has greater pozzolanicity (15%) than rice husk ash.

➢ Fresh properties results showed that the lowest workability and density were obtained by the lime mortar. The incorporation of silica fume and rice husk ash increased the flowability of lime mortar. The compressive strength of lime and lime composite mortars increases with curing age. Lime composite mortars performed better than pure lime mortar—four times the greater strength achieved. This is because the combined process of pozzolanic reaction and hydration leads to higher strength. The addition of cement (20%) to the lime composite mortars increased the early strength (7 days) to 250% and decreased the setting time to 50%. Higher water demand and air curing of lime mortar leads to higher shrinkage and water absorption. Lime composite mortar has 20% lower shrinkage and 40% lower water absorption than pure lime mortar.

➢ SEM-EDX and XRD analyses of lime mortar revealed the formation of thick white calcite granules in the microstructure, and carbonation of lime mortar was not completed at the period of 28 days. The microstructure of lime composite mortars showed a dense spherical morphology, and there was no any formation of acicular and hexagonal morphologies in the mortar. Quartz, calcium carbonate, calcium hydroxide and calcium silicate hydrate were the major peaks observed in the XRD of lime composite mortars. FT-IR graph of lime mortar confirmed the lime carbonation. A similar pattern in FT-IR graphs of lime composite mortars indicated the similar formation of hydration products.

➢ Overall, LSR (lime-silica fume) mortar exhibited a higher strength, workability and well-developed microstructure than other composite mortars.

➢ By considering all parameters, lime composite mortars can be effectively used in place of lime mortar for higher efficiency and performance. Further, the study was carried out using different secondary cementitious materials with lime for the production of

effective mortar or concrete that conserve the use of cement as well as the systematic use of lime.

## References

1. Thirumalini, S.; Ravi, R.; Rajesh, M. Experimental investigation on physical and mechanical properties of lime mortar: Effect of organic addition. *J. Cult. Herit.* **2018**, *31*, 97–104. [CrossRef]
2. Emayan, R.; Rahuman, S.A. Study on the compressive strength of lime mortar using admixtures. *Int. J. Innov. Res. Eng. Manag.* **2015**, *3*, 201–203.
3. Venugopal, B.; Manivannan, M.; Vigneshwaran, K.V.; Surya, S.; Thilagar, T. Study on the Performance Enhancement of Lime Mortar. *Int. J. Eng. Res. Technol.* **2018**, *6*, 1–3. [CrossRef]
4. Dhilipkumar, B.; Karthick, M.D. Experimental Study on Lime Mortar using Flyash and Gallnut as Additives. *Int. J. Eng. Res. Technol.* **2016**, *19*, 329–340.
5. Silva, B.A.; Pinto, A.P.F.; Gomes, A. Influence of natural hydraulic lime content on the properties of aerial lime-based mortars. *Constr. Build. Mater.* **2014**, *72*, 208–218. [CrossRef]
6. Zhang, D.; Zhao, J.; Wang, D.; Xu, C.; Zhai, M.; Ma, X. Comparative study on the properties of three hydraulic lime mortar systems: Natural hydraulic lime mortar, cement-aerial lime-based mortar and slag-aerial lime-based mortar. *Constr. Build. Mater.* **2018**, *186*, 42–52. [CrossRef]
7. Kadum, N.; al-Attar, T.; Al-Azzawi, Z. Evaluation of pozzolime mixtures as a sustainable binder to replace portland cement in structural concrete. In *MATEC Web of Conferences*; EDP Sciences: Ulys, France, 2017; Volume 120, p. 02009. [CrossRef]
8. Salman, M.M. The mechanical properties of Lime Concrete. *J. Eng. Sustain. Dev.* **2017**, *21*, 180–191.
9. Pavlik, V.; Uzakova, M. Effect of curing conditions on the properties of lime, lime–metakaolin and lime–zeolite mortars. *Constr. Build. Mater.* **2016**, *102*, 14–25. [CrossRef]
10. Cachim, P.; Velosa, A.L.; Rocha, F. Effect of Portuguese metakaolin on hydraulic lime concrete using different curing conditions. *Constr. Build. Mater.* **2010**, *24*, 71–78. [CrossRef]
11. Grist, E.R.; Paine, K.A.; Heath, A.; Norman, J.; Pinder, H. Structural and durability properties of hydraulic lime–pozzolan concretes. *Cem. Concr. Compos.* **2015**, *62*, 212–223. [CrossRef]
12. Velosa, A.L.; Cachim, P.B. Hydraulic-lime based concrete: Strength development using a pozzolanic addition and different curing conditions. *Constr. Build. Mater.* **2009**, *23*, 2107–2111. [CrossRef]
13. Pavía, S.; Walker, R.; Veale, P.; Wood, A. Impact of the Properties and Reactivity of Rice Husk Ash on Lime Mortar Properties. *Am. Soc. Civ. Eng.* **2014**, *26*, 04014066. [CrossRef]
14. Gleize, P.J.P.; Muller, A.; Roman, H.R. Microstructural investigation of a silica fume–cement-lime mortar. *Cem. Concr. Compos.* **2003**, *25*, 171–175. [CrossRef]
15. Latif, M.A.; Naganathan, S.; Razak, H.A.; Mustaphab, K.N. Performance of lime kiln dust as cementitious material. In Proceedings of the 5th International Conference of Euro Asia Civil Engineering Forum (EACEF-5), Procedia Engineering, Surabya, Indonesia, 15–18 September 2015; Volume 125, pp. 780–787. [CrossRef]
16. Grist, E.R.; Paine, K.A.; Heath, A.; Norman, J.; Pinder, H. Compressive strength development of binary and ternary lime—Pozzolan mortars. *Mater. Des.* **2013**, *52*, 514–523. [CrossRef]
17. Lee, H.; Vimonsatit, V.; Chindaprasirt, P.; Boonserm, K. Preliminary study of lime-pozzolan based cement after exposed to high temperatures. *Int. J. Adv. Agric. Environ. Eng.* **2014**, *1*, 6–12.
18. Nunes, C.; Slížková, Z.; Stefanidou, M.; Němeček, J. Microstructure of lime and lime-pozzolana pastes with nanosilica. *Cem. Concr. Compos.* **2016**, *83*, 152–163. [CrossRef]
19. Medina, C.; Bosque, I.F.S.D.; Frías, M.; Rojas, M.I.S.D. Design and characterisation of ternary cements containing rice husk ash and fly ash. *Constr. Build. Mater.* **2018**, *187*, 65–76. [CrossRef]

20. Kalagri, A.; Karatasios, I.; Kilikoglou, V. The effect of aggregate size and type of binder on microstructure and mechanical properties of NHL mortars. *Constr. Build. Mater.* **2014**, *53*, 467–474. [CrossRef]
21. Metwally, A.A.; Elaty, A.; Ghazy, M.F. Performance of Portland cement mixes containing silica fume and mixed with lime-water. *HBRC J.* **2014**, *10*, 247–257.
22. *IS 6932*; Laboratory Tests on Building Lime. Bureau of Indian Standards: New Delhi, India, 1973.
23. *IS 712*; Specification for Building Limes. Bureau of Indian Standards: New Delhi, India, 1984.
24. Olutoge, F.A.; Adesina, P.A. Effects of rice husk ash prepared from charcoal-powered incinerator on the strength and durability properties of concrete. *Constr. Build. Mater.* **2019**, *196*, 386–394. [CrossRef]
25. Nair, D.G.; Fraaij, A.; Klaassen, A.A.; Kentgens, A.P. A structural investigation relating to the pozzolanic activity of rice husk ashes. *Cem. Concr. Res.* **2008**, *38*, 861–869. [CrossRef]
26. *IS 269*; Code of Practice for Chemical and Physical Requirements of 33, 43, 53, 43S and 53S Grades of Ordinary Portland Cement. Bureau of Indian Standards: New Delhi, India, 2015.
27. *IS 383*; Specification for Coarse and Fine Aggregates from Natural Sources for Concrete. Bureau of Indian Standards: New Delhi, India, 1970.
28. *IS 2250*; Code of Practice for Preparation and Use of Masonry Mortars. Bureau of Indian Standards: New Delhi, India, 1981.
29. *IS 1727*; Methods of Test for Pozzolanic Materials. Bureau of Indian Standards: New Delhi, India, 1967.
30. *ASTM C 311-05*; Standard Test Methods for Sampling and Testing Fly Ash or Natural Pozzolans for Use in Portland-Cement Concrete. American Society for Testing and Materials: West Conshohocken, PA, USA, 2005.
31. *ASTM C 1240-03a*; Standard Specification for Silica Fume Used in Cementitious Mixtures. American Society for Testing and Materials: West Conshohocken, PA, USA, 2003.
32. *IS 4031-10*; Methods of Physical Tests for Hydraulic Cement, Part 10: Determination of Drying Shrinkage. Bureau of Indian Standards: New Delhi, India, 1988.
33. *ASTM C 642-06*; Standard Test Method for Density, Absorption, and Voids in Hardened Concrete. American Society for Testing and Materials: West Conshohocken, PA, USA, 2006.
34. Hemapriya, V.; Prabakaran, M.; Parameswari, K.; Chitra, S.; Kim, S.H.; Chung, I.M. Experimental and theoretical studies on inhibition of benzothiazines against corrosion of mild steel in acidic medium. *Anti-Corros. Methods Mater.* **2017**, *64*, 306–314. [CrossRef]
35. Chung, I.M.; Kim, S.H.; Prabakaran, M. Evaluation of phytochemical, polyphenol composition and anti-corrosion capacity of *Cucumis anguria* L. leaf extract on metal surface in sulfuric acid medium. *Prot. Met. Phys. Chem. Surf.* **2020**, *56*, 214–224. [CrossRef]
36. Malathy, R.; Prabakaran, M.; Kalaiselvi, K.; Chung, I.M.; Kim, S.H. Comparative polyphenol composition, antioxidant and anticorrosion properties in various parts of *Panax ginseng* extracted in different solvents. *Appl. Sci.* **2021**, *11*, 93. [CrossRef]
37. Malathy, R.; Arivoli, M.; Chung, I.M.; Prabakaran, M. Effect of surface-treated energy optimized furnace steel slag as coarse aggregate in the performance of concrete under corrosive environment. *Constr. Build. Mater.* **2021**, *284*, 122840. [CrossRef]
38. Chung, I.M.; Malathy, R.; Priyadharshini, R.; Hemapriya, V.; Kim, S.H.; Prabakaran, M. Inhibition of mild steel corrosion using *Magnolia kobus* extract in sulphuric acid medium. *Mater. Today Commun.* **2020**, *25*, 101687. [CrossRef]
39. Prabakarana, M.; Kim, S.H.; Kalaiselvi, K.; Hemapriya, V.; Chung, I.M. Highly efficient *Ligularia fischeri* green extract for the protection against corrosion of mild steel in acidic medium: Electrochemical and spectroscopic investigations. *J. Taiwan Inst. Chem. Eng.* **2016**, *59*, 553–562. [CrossRef]
40. Prabakaran, M.; Kim, S.H.; Hemapriya, V.; Chung, I.M. *Tragia plukenetii* extract as an eco-friendly inhibitor for mild steel corrosion in HCl 1 M acidic medium. *Res. Chem. Intermed.* **2016**, *42*, 3703–3719. [CrossRef]
41. Prabakaran, M.; Kim, S.H.; Hemapriya, V.; Gopiraman, M.; Kim, I.S.; Chung, I.M. *Rhus verniciflua* as a green corrosion inhibitor for mild steel in 1 M $H_2SO_4$. *RSC Adv.* **2016**, *6*, 57144–57153. [CrossRef]
42. Malathy, R.; Karuppasamy, N.; Prabakaran, M. Performance of prestressed concrete beams using magnetic water for concrete mixing. *J. Adhes. Sci. Technol.* **2022**, *36*, 666–684. [CrossRef]
43. Hemapriya, V.; Chung, I.M.; Kim, S.H.; Prabakaran, M. Inhibitory effect of biowaste on copper corrosion in 1 M HCl solution. *Mater. Today Commun.* **2021**, *27*, 102249. [CrossRef]
44. Walker, R.; Pavía, S. Physical properties and reactivity of pozzolans, and their influence on the properties of lime–pozzolan pastes. *Mater. Struct.* **2011**, *44*, 1139–1150. [CrossRef]
45. Mehta, P.K. Rice husk ash: A unique supplementary cementing material. In Proceedings of the International Symposiumon Advances in Concrete Technology, CANMET, Athens, Greece, 11–12 May 1992; pp. 407–430.
46. *ASTM C270*; Standard Specification for Mortar for Unit Masonry. American Society for Testing and Materials: West Conshohocken, PA, USA, 2014.
47. Adesina, P.A.; Olutoge, F.A. Structural properties of sustainable concrete developed using rice husk ash and hydrated lime. *J. Build. Eng.* **2019**, *25*, 100804. [CrossRef]
48. Ganesan, K.; Rajagopal, K.; Thangavel, K. Rice husk ash blended cement: Assessment of optimal level of replacement for strength and permeability properties of concrete. *Constr. Build. Mater.* **2008**, *22*, 1675–1683. [CrossRef]
49. Kumar, D.N.; Kumar, P.R. Investigations on alternate lime-pozzolana based mortars for repair of heritage structures. *Constr. Build. Mater.* **2022**, *341*, 127776. [CrossRef]

50.   Khatib, J.; Ramadan, R.; Ghanem, H.; Elkordi, A.; Baalbaki, O.; Kirgiz, M. Chemical shrinkage of paste and mortar containing limestone fines. *Mater. Today Proc.* **2022**, *61*, 530–536. [CrossRef]

51.   Khatib, J.; Ramadan, R.; Ghanem, H.; Elkordi ASonebi, M. Effect of limestone fines as a partial replacement of cement on the chemical, autogenous, drying shrinkage and expansion of mortars. *Mater. Today Proc.* **2022**, *58*, 1199–1204. [CrossRef]

52.   Khatib, J.; Ramadan, R.; Ghanem HElkordi, A. Effect of using limestone fines on the chemical shrinkage of pastes and mortars. *Environ. Sci. Pollut. Res.* **2022**, 1–12. [CrossRef]

53.   Khatib, J.; Ramadan, R.; Ghanem, H.; Elkordi, A. Volume stability of pastes containing limestone fines. *Buildings* **2021**, *11*, 366. [CrossRef]

54.   Jayasingh, S.; Baby, J. Influence of organic addition on strength and durability of lime mortar prepared with clay aggregate. *Mater. Today Proc.* **2022**. [CrossRef]

55.   Horgnies, M.; Chen, J.J.; Bouillon, C. Overview about the use of Fourier Transform Infrared spectroscopy to study cementitious materials. *WIT Trans. Eng. Sci.* **2013**, *77*, 251–262.

56.   Stuart, B.H. *Infrared Spectroscopy: Fundamentals and Applications*; John Wiley & Sons, Ltd.: Hoboken, NJ, USA, 2004.